VIA MEDICA

ORIGINAL ARTICLE

Cardiology Journal
2011, Vol. 11, No. 1, pp. 26–32

ISSN 1897–5593

Fractal dimensions of skin microcirculation flow in subjects with familial predisposition or newly diagnosed hypertension

Barbara Gryglewska[1], Mirosław Nęcki[1], Marcin Żelawski[2], Marcin Cwynar[1], Tomasz Baron[1], Marian Mrozek[2], Tomasz Grodzicki[1]

[1]Department of Internal Medicine and Gerontology, Medical College, Jagiellonian University, Cracow, Poland
[2]Institute of Computer Science, Jagiellonian University, Cracow, Poland

Abstract

Background: *Fractal analysis has been shown to be capable of characterizing irregular time series generated in non-linear systems. Fluctuations in skin flow signals have a fractal nature, but to date there has been no analysis of subjects with hypertension. The aim of this study is to assess the fractal dimensions of skin microcirculation flows in subjects with a familial predisposition or newly diagnosed hypertension.*

Methods: *A four-minutes rest flow (RF), minimal flow (BZ) during three-minutes ischemia and eight-minutes heat flow (HF) were recorded (using laser Doppler flowmetry) in patients with untreated hypertension, and in normotensives with no [NT(–)] or with a familial predisposition to hypertension [NT(+)]. Average one-minute surface areas under the curve of flow records and box dimensions (D) were calculated. Anova Kruskall-Wallis, χ^2 statistic and multivariate reverse regression analysis were used for calculation.*

Results: *We studied 70 people (average age 36.1 ± 10.3 years, 39 men). Hypertensives (n = 31) had significantly higher values of both clinical blood pressure and 24-hour ambulatory blood pressure, body mass index, glucose, triglycerides and insulin than the NT(–), (n = 17) and NT(+), (n = 22) groups. Mean values of flows and surface area under the curve of RF, BZ, HF records, D RF and D HF were comparable in studied groups, but D BZ differed (1.13 ± ± 0.05* vs *1.15 ± 0.05* vs *1.11 ± 0.05, respectively; p = 0.04). A family history of hypertension, insulin level and variability of 24-hour diastolic blood pressure were significant predictors of D BZ lower values in the multiple regression model.*

Conclusions: *Subjects with a familial predisposition to hypertension reveal altered homeodynamics of microvascular flow, with diminished chaotic ischemic flow.* (Cardiol J 2011; 18, 1: 26–32)

Key words: fractal dimension, skin microcirculation, laser Doppler flowmetry, hypertension, family predisposition

Address for correspondence: Barbara Gryglewska, MD, PhD, Department of Internal Medicine and Gerontology CM UJ, Śniadeckich 10, 31–531 Kraków, Poland, tel: +48 12 424 88 00, fax: +48 12 424 88 54, e-mail: bgrygle@su.krakow.pl

Received: 09.04.2010 Accepted: 11.06.2010

Introduction

Blood flow shows pronounced temporal variability which is a consequence of local changes in vasomotor activity, cardiac pulsations, vasomotion and the influence of the autonomic system on vascular tone [1, 2]. Skin flowmotion may be simply recorded by laser Doppler flowmetry (LDF). Interpreting LDF signals behavior has mainly involved using simple indices such as mean and standard deviation of flux [3]. However, flow oscillations, as with many physiological parameters, reveal non-linear instabilities, which may be better characterized by other methods. These so-called 'homeodynamics' [4] of LDF signals have been investigated using frequency domain methods based on the Fourier transform [5] and wavelet analysis [6]. Fluctuation of LDF signals has been also assessed by fractal analysis [7, 8]. That technique has been proven capable of characterizing irregular time series generated in non-linear systems, and may provide more valuable physiological insights than standard linear statistical measures [9]. Furthermore, it has been suggested that fractal models give the best description of reality [10]. A defining feature of healthy function is adaptability, the capacity to respond to unpredictable stimuli and stresses [11]. Fractal physiology may be adaptive; the absence of a characteristic scale inhibits the emergence of highly periodic behaviors, which would greatly narrow functional responsiveness.

Very many different types of fractal dimension have been described [12], but many are only applicable to pure mathematical fractal objects. The three most commonly used methods in biological science are the box-counting dimension [13], the perimeter stepping (or divider) dimension [14] and the pixel dilation method [15]. The fractal dimension of time series may also be determined by dispersional analysis [8]. The box-counting dimension is the easiest to implement. In medicine, fractal analysis has been used to describe the anatomy of the arterial and venous trees, the branching of certain cardiac muscle bundles, as well as the ramifying tracheobronchial tree and His-Purkinje network, nervous system, bowel, biliary duct system and renal calyces [11]. Moreover, complex fluctuations with the statistical properties of fractals have been described for heart-rate variability, fluctuations in respiration, systemic blood pressure, human gait, white blood cell counts, as well as certain ion-channel kinetics [11].

It has been demonstrated that skin microcirculation flow also has a fractal character [7]. There has been no analysis of fractal dimension of LDF signals in hypertensive subjects. In the present study, we decided to analyze alterations of rest and reactive skin flow fractal dimensions (D) in normal subjects with, and without, a familial predisposition to hypertension, and in patients with newly diagnosed hypertension.

Methods

Study population

The experimental protocol has been approved by the local Ethics Committee at the Medical College of the Jagiellonian University and it conforms to the guidelines set out in the Declaration of Helsinki. Subjects were recruited into the study from ambulatory patients at the hypertensiology center and from healthy volunteers. Healthy subjects were divided into two groups according to family history of hypertension (one or both parents) as normotensives without [NT(–)] or with [NT(+)] a familial predisposition to hypertension. Hypertensive patients (HT) were newly diagnosed and untreated. All participants were free from further known cardiovascular risk factors or related comorbidities. Heavy smokers (more than five cigarettes per day) were excluded from the study.

Blood pressure measurements

Conventional blood pressure (BP) measurements and ambulatory blood pressure monitoring (ABPM) were performed on all study participants. Conventional BP measurements were conducted by the same investigator on the upper right arm with the cuff inflated at heart level using a mercury sphygmomanometer. Before the measurements, the subject remained in the supine position for about ten minutes and then underwent three blood pressure measurements at two-minute intervals. Systolic blood pressure (SBP) level was recorded at Korotkow Phase I and diastolic blood pressure (DBP) at Korotkow Phase V. Mean values of the two last measurements were used in further analysis.

ABPM was recorded over a working day using automatic SpaceLabs 90207 unit. The cuff with the appropriate bladder size was fixed to the studied arm, and the device was set to obtain automatic BP readings at 15-minute intervals during the daytime and at 30-minute intervals during the nighttime. Investigators performing ABPM were blinded to the clinical status of examined subjects. More than 80% of successful readings were required to qualify the test for subsequent analysis. The mean values and variability (expressed as standard deviation [SD]) of 24-hour SBP/DBP were analyzed.

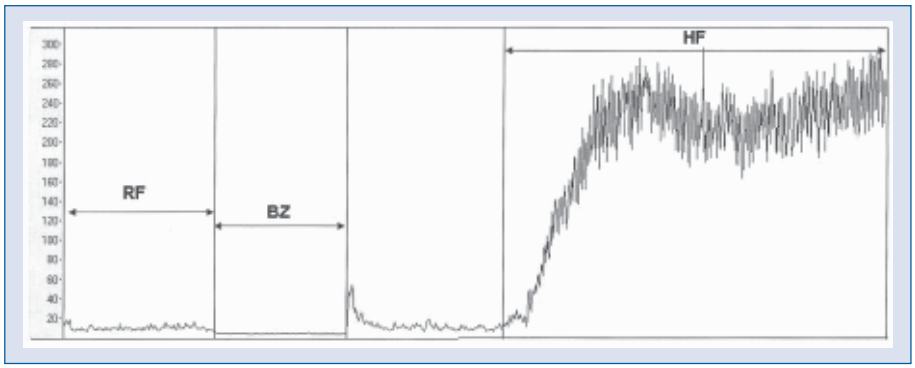

Figure 1. Compressed resting (RF), ischemic (BZ — biological zero) and heat (HF) flow records of laser Doppler flowmetry.

Laser Doppler flowmetry

All measurements were performed in the morning in a quiet room at temperatures of approximately 21–22°C. Subjects were asked to refrain from smoking and drinks containing caffeine on the day of examination. Skin blood flow was measured as cutaneous red blood cell flux using PeriFlux LDF. The LDF probe (Periflux System 5000, Perimed, Järfälla/Stockholm, Sweden) was attached (using an adhesive) to the right forearm to measure skin blood flow. The recording was performed after a 20-minute period of adjustment in the supine position, with LDF signal stable for approximately ten minutes before the recording. The day-to-day reproducibility of the flow has been demonstrated previously [16].

The LDF signal was recorded continuously (Fig. 1). A four-minute baseline resting flow was recorded prior to forearm ischemia which was produced by a pneumatic cuff, positioned at the arm and inflated to 50 mm Hg above the SBP of the studied person. A three-minute ischemic flow (biological zero) was registered. After cuff release and reversion of resting flow, the local heating units were heated from skin temperature to 44°C over 15–22 s and maintained at this temperature for eight minutes.

The following data was digitized and stored on the computer and analyzed off-line using signal processing software (PeriSoft 2.5.5, Perimed): mean values of four minutes resting blood flow (RF), three minutes flow of biological zero (BZ) and eight minutes heat flow (HF). The values of blood flow were expressed as absolute values (AU, arbitrary units).

The time series of original data of RF, BZ and HF flows were used for further calculations. The surface (S) under the curves was calculated as the sum of subareas enclosed by $x = T_i$, $x = T_{i+1}$. Average one-minute surface areas were calculated as the ratio $= S/(T_n–T_0)$. The algorithm of the box dimension (D) calculation utilized the series of measurements (T_0, M_0), (T_1, M_1),…(T_n, M_n). A rectangular area $[O=\{(x,y)\,|\,T_0<=x<=T_n$ and $0<=y<=h\}]$ containing the flow curve was covered with boxes (square grid) of size $k_0 = t_{min}$. The boxes $N(k_0)$ that contained any part of the flow curve were counted. This operation was repeated for the $k_1 = 2^* k_0$, $k_2 = 2^{2*}k_0$, ..., $k_{m-1} = 2^{(m-1)*}k_0$, where $k_{m-1} <= \min\{t_{max}, h, T_n–T_0\}$ and $k_m > \min\{t_{max}, h, T_n–T_0\}$. The box dimension was computed as the slope of a least-square regression line fit to the points $(\log k_i, \log N(k_i))$. The algorithms were implemented in the C# programming language.

Other measurements

Height and weight were measured, and body mass index (BMI) was calculated. Pulse wave velocity (PWV) between common carotid and femoral arteries was measured using a Complior device (Colson, France). The transit time between the carotid and the femoral pulse waves was automatically determined by the software and PWV was calculated as the ratio of distance between transducers and transit time. An echocardiogram was obtained in M mode (after selection of the measurement section by a B-mode scan), which allowed left ventricular mass index according to the formula proposed by the American Echocardiographic Society [17]. Venous blood samples were obtained from each participant after an overnight fast (from 6pm to 8am) to determine blood count, serum glucose, urea (BUN) and sodium levels and lipid profile (total cholesterol, triglyceride, LDL and HDL levels), according to established methods. Plasma osmolarity [mosm/L] was calculated according to the formula: $2[Na^+]$ + [glucose] + [BUN] in mmol/L. Part of the blood specimen was centrifuged

Table 1. Characteristics of the study groups.

	NT(–); n = 17	NT(+); n = 22	HT; n = 31	p
Age (years)	34.82 ± 13.88	34.2 ± 8.64	37.97 ± 9.19	
Male gender (%)	41.2	50.0	67.7	
Body mass index [kg/m^2]	22.03 ± 2.40	23.25 ± 2.72	25.30 ± 3.34***	0.002
Pulse wave velocity [m/s]	8.77 ± 1.79	7.73 ± 1.46	8.89 ± 2.14	
Insulin [μU/mL]	5.63 ± 1.69	7.50 ± 5.79	8.19 ± 3.33*	0.03
Glucose [mmol/L]	4.79 ± 0.52	4.91 ± 0.81	5.29 ± 0.70*	0.01
HOMA index	1.21 ± 0.44	1.82 ± 0.91	1.94 ± 0.82$^{\&}$	0.01
Triglyceride [mmol/L]	1.18 ± 0.49	1.24 ± 0.74	1.91 ± 1.27$^{\#}$	0.04
Total cholesterol [mmol/L]	5.07 ± 1.39	4.81 ± 0.74	5.25 ± 1.09	
High density lipoprotein [mmol/L]	1.54 ± 0.28	1.56 ± 0.57	1.30 ± 0.31	
Low density lipoprotein [mmol/L]	2.99 ± 1.34	2.73 ± 0.56	3.03 ± 1.03	
Hematocrit (%)	40.96 ± 2.77	40.74 ± 3.34	42.40 ± 2.68	
Osmolarity [mosm/L]	271.82 ± 9.34	268.02 ± 6.27	268.66 ± 5.20	
Left ventricular mass index [g/m^2]	114.6 ± 17.5	102.9 ± 13.9	119.2 ± 31.4 ^	0.05
Clinical SBP [mm Hg]	122.1 ± 11.5	121.3 ± 8.6	152.6 ± 8.3	< 0.001
Clinical DBP [mm Hg]	80.1 ± 6.3	75.4 ± 6.8	95.1 ± 6.9	< 0.001
24 h SBP [mm Hg]	118.2 ± 9.0	113.8 ± 6.9	132.6 ± 10.2	< 0.001
Variability of 24 h SBP [mm Hg]	12.7 ± 2.7	11.2 ± 2.9	13.1 ± 3.3	
24 h DBP [mm Hg]	72.9 ± 6.0	71.1 ± 4.7	83.2 ± 8.3	< 0.001
Variability of 24 h DBP [mm Hg]	10.9 ± 1.5	10.4 ± 2.2	11.3 ± 2.7	
24 h heart rate [beats/min]	72.1 ± 9.6	74.4 ± 7.5	79.0 ± 9.5**	0.05

*HT *vs* NT(–): p = 0.03; **HT *vs* NT(–): p = 0.06; ***HT *vs* NT(–): p = 0.002; $^{\#}$HT *vs* NT(+): p = 0.08; $^{\&}$HT *vs* NT(–): p = 0.01; ^ HT *vs* NT(+): p = 0.05; NT — normotensive subjects; (–) negative family history of hypertension; (+) positive family history of hypertension; HT — sustained hypertension; SBP — systolic blood pressure; DBP — diastolic blood pressure

and stored at –80°C for subsequent measure of insulin [μU/mL] using electrochemiluminescence immunoassay (Roche Elecsys 2010). The homeostasis model assessment (HOMA) index was obtained according to the following formula: (fasting plasma glucose × fasting plasma insulin)/22.5 [18].

Statistical analysis

Results were expressed as means ± SD. Between-group comparisons were made using the ANOVA Kruskall-Wallis test for nonparametric data with *post hoc* analysis to identify individual differences between groups, and using χ^2 test to investigate differences within categorical variables distribution. Analysis of covariance (ANCOVA) was used to adjust studied parameters for variables that are not comparable among the groups. Multivariate reverse regression analysis was used to detect the parameters of the study population, which can constitute predictors of skin flow fractal dimensions. The simplest significant model was selected. A p value < 0.05 was considered statistically significant.

Results

The study population consisted of 70 people (mean age 36.1 ± 10.3 years, 44.3% women): 17 NT(–), 22 NT(+), 31 HT, age and gender matched. Groups differed according to BMI, glucose, triglyceride, insulin levels, HOMA index and BP values (Table 1). HT patients had significantly higher values of BMI (p = 0.002), glucose (p = 0.01), insulin (p = 0.03) levels and also HOMA index (p = 0.01) and 24 hours heart rate (p = 0.06) than NT(–) subjects. Moreover, hypertensives presented higher triglyceride levels (p = 0.08) and left ventricular mass index (LVMI) (p = 0.05) than NT(+) normotensives. BP values were significantly higher in hypertensive as opposed to normotensive groups (*post hoc* analysis is not presented). Variability of 24 hour BP was similar among the studied groups. There were also observed typical gender differences of HDL cholesterol levels (women: 1.6 ± ± 0.5; men: 1.3 ± 0.4, p < 0,05) and LVMI (women: 102.8 ± 14.6; men: 121.9 ± 28.2, p < 005).

Table 2. Mean values of skin flows and average one-minute surface areas (AvS) under curve records in the study groups.

Parameters of flow*	NT(–); n = 17	NT(+); n = 22	HT; n = 31	p
RF [AU]	9.73 ± 3.82	8.84 ± 4.23	10.15 ± 3.88	
AvS RF [AU²/min]	9.78 ± 3.92	9.49 ± 4.5	9.97 ± 4.09	
BZ [AU]	4.6 ± 1.02	3.97 ± 1.1	4.34 ± 1.81	
AvS BZ [AU²/min]	4.7 ± 1.07	4.3 ± 1.6	4.47 ± 1.81	
HF [AU]	133.40 ± 46.37	98.53 ± 34.11	112.4 ± 45.11	
AvS HF [AU²/min]	124.3 ± 57.5	91.1 ± 26.8	109.6 ± 46.6	0.06

*Adjusted for body mass index; RF — rest flow; BZ — biological zero; HF — heat flow

The mean values of RF, BZ and HF were similar in all studied groups (Table 2). Average one-minute area under the curve of RF and BZ was also comparable in the groups, but we observed a tendency to lower values of area under the curve of HF in NT(+) subjects than in the others. Fractal dimensions (D) of RF and HF were similar, but of BZ differed among the studied groups (Fig. 2). The lowest values (1.11 ± 0.05) was detected in NT(+) subjects, and higher differences were observed with regard to the NT(–) group, (1.15 ± 0.06, p = 0.04) than the HT group (1.13 ± 0.05).

Multiple regression model included age, gender, family history of HT, BMI, PWV, values of clinical BP and ABPM measurements, hematocrit, osmolarity, fasting blood glucose, lipids and insulin levels as independent variables. Significant predictors of D BZ are presented in Table 3. A family history of HT, variability of 24 hour DBP and insulin level were significant predictors of D BZ reduction.

Discussion

The results revealed that a family predisposition to HT is connected to diminished values of fractal dimension of ischemic flow in skin microcirculation. A family history of HT, variability of 24 hour DBP and insulin level were significant predictors of that reduction.

The lower fractal dimension of microcirculation flow may point to its lower chaotic character. The chaotic fluctuations of flow confer greater stability to microcirculatory perfusion and may influence flow independently of their amplitude, as was shown based on the model of a single resistance vessel [19]. As chaotic patterns of vasomotion preserve a more homogeneous characteristic of perfusion, diminished fractal dimension of ischemic flow in our subjects with familial predisposition to HT might suggest weakening of skin ischemic flow in those persons. Studies of flowmotion in animal models of

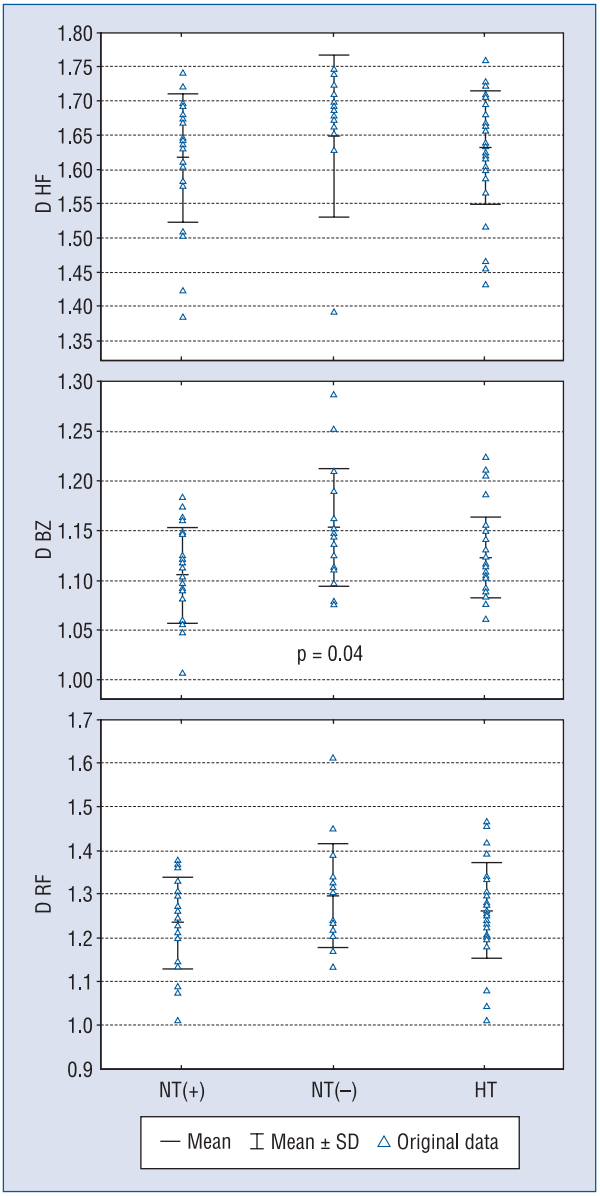

Figure 2. Fractal dimensions of resting (D RF), ischemic (D BZ) and heat (D HF) flows in study groups; NT — normotensive subjects; (–) negative family history of hypertension; (+) positive family history of hypertension; HT — sustained hypertension.

Table 3. Significant predictors of ischemic flow (biological zero) fractal dimension in multiple regression models.

Fractal dimension of ischemic flow (corrected $R^2 = 0.16$; $p < 0.02$)	β coefficient	p
Family history	–0.28	0.04
Hematocrit	0.26	0.10
Variability of 24 h diastolic blood pressure	–0.33	0.03
Total cholesterol	0.18	0.18
Insulin level	–0.38	0.01

HT have had inconsistent results. It has been observed that rhythmic activity was more prevalent in arteries from hypertensive rats than in normotensive controls [20] and spontaneous rhythmic activity in rat aorta appeared secondary to chronic pressure loading following experimental coarctation [21]. On the other hand, fluctuations in pressure and flow in renal proximal tubules were normally periodic, but became chaotic following the onset of HT [22]. It seems probable that results might be specific for different vascular trees and may be related to a genetic predisposition to HT, as our results suggest.

Mechanisms of chaotic flowmotion reduction may be structural or functional. Changes in structure of the vascular tree are thought to be the root cause of perfusion heterogeneity within different tissues [23]. It has been shown that capillary tortuosity, especially when combined with the increased number of capillary anastamoses, decreases perfusion heterogeneity [24]. The structural abnormalities were detected in HT but also in normotensive individuals with familial predisposition to HT [25, 26].

The vascular tree structure is inherently optimized for oxygen delivery [27]. However, observed differences in perfusion heterogeneity may be also due to differences in the physiological control mechanisms of perfusion. Skin microcirculatory flowmotion is controlled firstly by a combination of metabolic factors such as nitric oxide (NO) produced in response to endothelial cell shear stress; secondly by vascular smooth muscle activity which is proportional to the tissue's metabolic demand for oxygen; and thirdly by fluctuations in the ion concentrations, mainly Ca^{++}, across the membrane of vascular smooth muscle cells [1, 28–30]. Such mechanisms may be disturbed in many cardiovascular diseases. It is generally agreed that HT is accompanied by endothelial dysfunction, in which oxidant generation and uncoupling of endothelial NO syntase play an important role [31, 32]. Impaired vasodilation related to the endothelium has been confirmed not only in HT but also in many cardiovascular diseases, and may also precede its development, as shown in the study of the offspring of hypertensive patients [31–33].

The fractal character of flows in human hypertensives has not been investigated to date. However, there have been some fractal analyzes of retinal vessels structure in hypertensive patients. The fractal dimension of the retinal vascular network appeared smaller for hypertensives than for non-hypertensives [34]. Fractal analyzis of 24 hours blood pressure fluctuations did not reveal fractal character, but results suggested that the complexity of heart rate signal might be altered in HT [35]. In cardiology, several new analyzis methods of heart rate behavior, motivated by non-linear dynamics and chaos theory, have been developed to quantify the dynamics of heart rate fluctuations [11]. Complex heart rate fluctuations seen during normal sinus rhythm in healthy individuals, even at rest, are attributable in part to deterministic chaos. Various diseases, such as those associated with congestive heart failure syndromes, may involve a paradoxical decrease in this type of non-linear variability. Moreover, the reduced short-term fractal exponent of heart rate variability remains the independent predictor of mortality [36].

Our results showed for the first time that people with a familial predisposition to HT present diminished chaotic behavior of ischemic skin flow. A family history of HT, variability of 24 hour DBP and insulin level were significant predictors of that reduction. As chaotic patterns of vasomotion preserve the more homogeneous characteristics of perfusion, and simultaneously familial predisposition to HT constitutes an unmodifiable risk factor, modification of DBP characteristics and insulin level may have significance in protecting against weakening of skin ischemic flow. However, further studies are needed to estimate the fractal character of microcirculation flows, as well as the mechanism and clinical meaning of this phenomenon.

Acknowledgements

The authors do not report any conflict of interest regarding this work.

The research was supported by the Ministry of Science and Higher Education within the Contract No. 4P05B123.

References

1. Nilsson H, Aalkjaer C. Vasomotion: Mechanisms and physiological importance. Mol Interv, 2003; 3: 79–89.
2. Lamboley M, Schuster A, Bény JL, Meister JJ. Recruitment of smooth muscle cells and arterial vasomotion. Am J Physiol Heart Circ Physiol, 2003; 285: H562–H569.
3. Van den Brande P, von Kemp K, De Connick A, Debing E. Laser Doppler flux characteristics at the skin of the dorsum of the foot in young and in elderly healthy human subjects. Microvasc Res, 1997; 53: 156–162.
4. Yates FE. Homeokinetics/homeodynamics: A physical heuristic for life and complexity. Ecol Psychol, 2008; 20: 148–179.
5. Muck-Weymann ME, Albrecht HP, Hager D, Hiller D, Hornstein OP, Bauer RD. Respiratory-dependent laser-Doppler flux motion in different skin areas and its meaning to autonomic nervous control of the vessels of the skin. Microvasc Res, 1996; 52: 69–78.
6. Stefanovska A, Bracic M, Kvernmo HD. Wavelet analysis of oscillations in the peripheral blood circulation measured by laser Doppler technique. IEEE Trans Biomed Eng, 1999; 46: 1230–1239.
7. Carolan-Rees G, Tweddel AC, Naka KK, Griffith TM. Fractal dimensions of laser doppler flowmetry time series. Med Eng Phys, 2002; 24: 71–76.
8. Bassingthwaite JB, Raymond GM. Evaluation of dispersional analysis method for fractal time series. Ann Biomed Eng, 1995; 23: 491–505.
9. Wagner CD, Persson PB. Chaos in the cardiovascular system: An update. Cardiovasc Res, 1998; 40: 257–264.
10. Glass L. Synchronization and rhythmic processes in physiology. Nature, 2001; 410: 277–284.
11. Goldberger AL. Non-linear dynamics for clinicians: Chaos theory, fractals, and complexity at the bedside. Lancet, 1996; 347: 1312–1314.
12. Cross SS. The application of fractal geometric analysis to microscopic images. Micron, 1994; 25: 101–113.
13. Glenny RW, Robertson HT, Yamashiro S, Bassingthwaighte JB. Applications of fractal analysis to physiology. J Appl Physiol, 1991; 70: 2351–2367.
14. Sanders H, Crocker J. A simple technique for the measurement of fractal dimensions in histopathological specimens. J Pathol, 1993; 169: 383–385.
15. Wingate RJ, Fitzgibbon T, Thompson ID. Lucifer yellow, retrograde tracers, and fractal analysis characterize adult ferret retinal ganglion cells. J Comp Neurol, 1992; 323: 449–474.
16. Grodzicki T, Necki M, Cwynar M, Gryglewska B. Laser Doppler flowmetry: Repeatability of the method (in Polish). Przegl Lek, 2003; 60: 89–91.
17. Cheitlin MD, Armstrong WF, Aurigemma GP et al. ACC/AHA/ /ASE 2003 guideline update for the clinical application of echocardiography: summary article: A report of the American College of Cardiology/American Heart Association Task Force on Practice Guidelines (ACC/AHA/ASE Committee to Update the 1997 Guidelines for the Clinical Appl ication of Echocardiography). Circulation, 2003; 108: 1146–1162.
18. Matthews DR, Hosker JP, Rudenski AS, Naylor BA, Treacher DF, Turner RC. Homeostasis model assessment: insulin resistance and beta-cell function from fasting plasma glucose and insulin concentrations in man. Diabetologia, 1985; 28: 412–419.
19. Parthimos D, Edwards DH, Griffith TM. Comparison of chaotic and sinusoidal vasomotion in the regulation of microvascular flow. Cardiovasc Res, 1996; 31: 388–399.
20. Mulvany MJ. Possible role of vascular oscillatory activity in the development of high blood pressure in spontaneously hypertensive rats. J Cardiovasc Pharmacol, 1988; 12 (suppl. 6): S16–S20.
21. White CR, Zehr JE. Spontaneous rhythmic contractile behaviour of aortic ring segments isolated from pressure loaded regions of the vasculature. Cardiovasc Res, 1990; 24: 953–958.
22. Holstein-Rathlou N-H, Marsh DJ. Renal blood flow regulation and arterial pressure fluctuations: A case study in nonlinear dynamics. Physiol Rev, 1994; 74: 637–681.
23. Beard DA, Bassingthwaighte JB. The fractal nature of myocardial blood flow emerges from a whole-organ model of arterial network. J Vasc Res, 2000; 37: 282–296.
24. Goldman D, Popel AS. A computational study of the effect of capillary network anastomoses and tortuosity on oxygen transport. J Theor Biol, 2000; 206: 181–194.
25. Noon JP, Walker BR, Webb DJ et al. Impaired microvascular dilatation and capillary rarefaction in young adults with a predisposition to high blood pressure. J Clin Invest, 1997; 99: 1873–1879.
26. Antonios TF, Rattray FM, Singer DR, Markandu ND, Mortimer PS, MacGregor GA. Rarefaction of skin capillaries in normotensive offspring of individuals with essential hypertension. Heart, 2003; 89: 175–178.
27. Baba K, Kawamura T, Shibata M, Sohirad M, Kamiya A. Capillary-tissue arrangement in the skeletal muscle optimized for oxygen transport in all mammals. Microvasc Res, 1995; 49: 163–179.
28. Koenigsberger M, Sauser R, Beny J-L, Meister J-J. Role of the endothelium on arterial vasomotion. Biophys J, 2005; 88: 3845–3854.
29. Haddock RE, Hill CE. Rhythmicity in arterial smooth muscle. J Physiol, 2005; 566: 645–656.
30. Lamboley M, Schuster A, Bény JL, Meister JJ. Recruitment of smooth muscle cells and arterial vasomotion. Am J Physiol Heart Circ Physiol, 2003; 285: H562–H569.
31. Levy BI, Ambrosio G, Pries AR, Struijker-Boudier HA. Microcirculation in hypertension: A new target for treatment? Circulation, 2001; 104: 735–740.
32. Endemann DH, Schiffrin EL. Endothelial dysfunction. J Am Soc Nephrol, 2004; 15: 1983–1992.
33. Taddei S, Salvetti A. Pathogenetic factors in hypertension. Endothelial factors. Clin Exp Hypertens, 1996; 18: 323–335.
34. Liew G, Wang JJ, Cheung N et al. The retinal vasculature as a fractal: Methodology, reliability and relationship to blood pressure. Ophthalmology, 2008; 115: 1951–1956.
35. Lanteime P, Milon H, Charib C, Tremeau G, Fortrat J-O. Analyse fractale et hypertension arterielle. Arch Mal Coeur Vaiss, 1999; 92: 1121–1125.
36. Mäkikallio TH, Huikuri HV, Hintze U et al. Fractal analysis and time- and frequency-domain measures of heart rate variability as predictors of mortality in patients with heart failure. Am J Cardiol, 2001; 87: 178–182.